Enhanced Visible Light Absorption for Lead-free Double Perovskite $Cs_2AgSbBr_6$

Fengxia Wei,[a,b] Zeyu Deng,[b] Shijing Sun,[c] Noor Titan Putri Hartono,[c] Debbie Seng,[a] Tonio Buonassisi,[c#] Paul D. Bristowe,[b] Anthony K. Cheetham[b,d]

[a] Institute of Materials Research and Engineering, A*STAR, 2 Fusionopolis Way, Innovis, Singapore 138634
[b] Department of Materials Science and Metallurgy, University of Cambridge, Cambridge CB3 0FS, UK
[c] Department of Mechanical Engineering, Massachusetts Institute of Technology, Massachusetts 02139, USA
[d] Department of Materials Science and Engineering, National University of Singapore, Singapore 117575.
[#]On leave to Institute of Materials Research and Engineering, A*STAR, 2 Fusionopolis Way, Innovis, Singapore 138634

Table of contents

List of tables and figures

Synthesis

$Cs_2AgSbBr_6$ crystal. Single crystals were synthesised by the hydrothermal method using 1 mmol CsBr, 0.5 mmol AgBr and 0.5 mmol $SbCl_3$ with 0.5 ml HBr acid (47wt%) in a 23 ml stainless steel Parr autoclave at 160°C for 5 days.

$Cs_2AgSbBr_6$ film/ device. A TiO_2 compact layer is deposited on a FTO substrate using titanium diisopropoxide bis(acetylacetonate) 75% wt. (Sigma-Aldrich) precursor mixed in ethanol, with the spray pyrolysis method. After sintering at 500°C, a TiO_2 mesoporous solution (SureChem, SC-HT040) is spincoated onto the substrate and sintered at the same temperature. The perovskite precursor solution is made by mixing 0.179 g CsBr powder (Alfa Aesar) with 0.079 g AgBr powder (Sigma-Aldrich). Then, 700 µL of 0.6 M $SbBr_3$ (Alfa Aesar) in DMSO is added to the precursors for the $Cs_2AgSbBr_6$ perovskite precursor solution. Before depositing the layer, both substrate and precursor solution are preheated to 200°C, and 100 µL of the solution is spincoated at 6000 rpm speed for 30 seconds, with no anti-solvent. After that, the substrate with the thin film is annealed for 30 minutes at 150°C to evaporate the leftover solvent. The hole-transport layer deposited next is spiro-OMeTAD (LumTec LT-S922), doped with LiTFSI, FK209 Co(III) TFSI salt, and TBP. Finally, the 100 nm gold contact is deposited using a thermal evaporator.

$Cs_2AgBiBr_6$ film. Using a glass slide as a substrate, a perovskite precursor solution made of 0.254 CsBr powder (Alfa Aesar), 0.113 AgBr (Sigma-Aldrich), and 0.268 g $BiBr_3$ (Sigma-Aldrich) mixed in 1 mL DMSO was prepared based on the literature method.[2] Before depositing the layer, both substrate and precursor solution are preheated to 75°C, and 100 µL of the precursor solution is spincoated at 6000 rpm speed for 30 seconds, with no anti-solvent. Finally, it is annealed for 30 minutes at 285°C to evaporate the leftover solvent.

X-ray diffraction

Crystal structure determination was carried out using an Oxford Gemini E Ultra diffractometer, Mo Kα radiation (λ = 0.71073 Å), equipped with an Eos CCD detector. Various temperature diffractions were carried out by collecting data from 300 K to 120 K using a Cryo system under liquid nitrogen flow with 50 K steps, then heated up to 400 K; the crystal stayed under nitrogen flow for 10 mins at each temperature, allowing sufficient time for cooling. Data collection and reduction were conducted using CrysAliPro. An empirical absorption correction was applied with the Olex2 platform, and the structure was solved using ShelXS[1] and refined with ShelXL.[2] For thin-film samples, a SmartLab X-ray powder diffractometer with a Cu K-α radiation source was employed at ambient conditions. XRD patterns of 2-Theta/ Omega scans were collected from 5-60°.

X-ray photoelectron spectroscopy

XPS analysis was performed using a Thermo Scientific Theta Probe XPS with a monochromatic Al Kα X-ray source (hν=1486.7 eV) at incident angle of 30° with respect to the surface normal. Photoelectrons were collected at a take-off angle of 50° with respect to the surface normal. Charge correction was referenced to adventitious carbon C 1s at 285.0 eV. X-

ray spot size 400 μm in diameter was used and survey scan was conducted at step of 1 eV with pass energy 200 eV, the narrow scans were at 0.1 eV steps with pass energy = 40 eV.

UV-Vis spectroscopy

Optical measurements were carried out on a PerkinElmer Lambda 750 UV-Visible spectrometer in the reflectance mode with a 2nm slit width. The scan interval was 1 nm and the scan range was between 300 and 1300nm.

X-ray Fluorescence

XRF on single crystals was conducted with Rh Kα radiation on an M4 TORNADO spectrometer with a beam size of 25μm and a 100s dwelling time.

Density Function Theory Calculations

DFT calculations were performed using projected augmented wave (PAW) pseudopotentials[3,4] as implemented in the *Vienna Ab initio Simulation Package* (VASP) code.[5,6] The following electrons were treated explicitly: Cs $5s^2 5p^6 6s^1$, Ag $4p^6 4d^{10} 5s^1$, Sb $5s^2 5p^3$, Bi $5d^{10} 6s^2 6p^3$ and Br $4s^2 4p^7$. The optB86b-vdW exchange-correlation functional was employed.[7] A 500 eV kinetic energy cut-off as well as a Γ-centered $4 \times 4 \times 4$ Monkhorst-Pack k-point sampling were used.[8] All structures (primitive cell) were optimised until the interatomic forces were less than 0.01 eV/Å. The electronic band structures and density of states (DOS) were calculated using the HSE06 hybrid functional and considering spin-orbit coupling (SOC).[9] For the DOS calculation, a denser $5 \times 5 \times 5$ k-point mesh was used. The carrier effective masses were fitted from valence and conduction band eigenvalues using a parabolic model. The mechanical properties were calculated from the stress-strain relationship by applying e_1+e_4 $(\delta\ 0\ 0\ \delta\ 0\ 0)$ strains using 0%, ±0.5%, and ±1% deformations.[10] The Quantum Theory of Atom-in-Molecules (QTAIM) analysis[11] was performed using the CRITIC2 code.[12]

DFT structural relaxation showed that $Cs_2AgSbBr_6$ possesses a lattice parameter of 11.1602 Å whereas $Cs_2AgBiBr_6$ is slightly larger (11.2612 Å). This is expected because the ionic radius of Bi (103 pm) is larger than Sb (76 pm). The DFT calculated formation enthalpies show that $Cs_2AgSbBr_6$ is thermodynamically less stable than $Cs_2AgBiBr_6$ (40.09 kJ/mol per f.u.). This is supported by the observation that $Cs_2AgBiBr_6$ is much easier to synthesize experimentally.

Table S1. Comparison of DFT calculated and experimental lattice constants (Å) of $Cs_2AgSbBr_6$ and $Cs_2AgBiBr_6$.

	$Cs_2AgSbBr_6$	$Cs_2AgBiBr_6$
DFT	11.1602	11.2612
Exp	11.1583	11.2499[13]

The DFT calculated elastic constants and moduli (Table 3 and Table 4) show that $Cs_2AgSbBr_6$ is mechanically stiffer than $Cs_2AgBiBr_6$. A QTAIM analysis[10] of charge densities was performed to probe the bond strengths of $Cs_2AgSbBr_6$ and $Cs_2AgBiBr_6$. In the analysis the charge density (ρ) at the bond critical point (BCP) indicates the relative bond strength and the Laplacian ($\nabla^2\rho$) shows whether the charge is concentrated (< 0) or depleted (> 0). From the results (Table 5), we can see that at the BCP, ρ is larger between Sb-Br than Bi-Br, suggesting that Bi-Br bonds are more compliant than Sb-Br. In addition, positive values of $\nabla^2\rho$ indicate that Ag-Br and Sb/Bi-Br bonds have ionic character. Also, $Cs_2AgSbBr_6$ has a smaller inorganic cage as indicated by its lattice constant which leads to a more significant steric effect of Cs within $Cs_2AgSbBr_6$. This further affects the stiffness of the structures. Therefore, a stronger bonding between Sb-Br than Bi-Br as well as a more close-packed cage makes $Cs_2AgSbBr_6$ a mechanically stronger material. Both $Cs_2AgBiBr_6$ and $Cs_2AgSbBr_6$ have larger elastic moduli than the previously reported hybrid perovskite systems $(MA)_2KBiCl_6$, $(MA)_2TlBiBr_6$ and $(MA)_2AgBiBr_6$.[9,15,16]

Table S2. DFT calculated elastic constants of $Cs_2AgSbBr_6$ and $Cs_2AgBiBr_6$. Units are in GPa.

	c_{11}	c_{12}	c_{44}
$Cs_2AgBiBr_6$	47.56	15.7	8.19
$Cs_2AgSbBr_6$	51.04	18.58	8.91

Table S3. DFT calculated polycrystalline Young's modulus (E), shear modulus (G), bulk modulus (B) and Poisson's ratio (ν) of $Cs_2AgSbBr_6$ and $Cs_2AgBiBr_6$. Except ν, which is dimensionless, all units are in GPa.

	E	G	B	ν
$Cs_2AgBiBr_6$	28.34	10.73	26.32	0.32
$Cs_2AgSbBr_6$	30.18	11.35	29.4	0.33

Table S4. Charge densities ρ (e/Å^3) and Laplacian $\nabla^2\rho$ (e/Å^5) at the bond critical point (BCP) for Ag-Br and Sb/Bi-Br bonds of $Cs_2AgSbBr_6$ and $Cs_2AgBiBr_6$ from QTAIM analysis.

	$Cs_2AgSbBr_6$		$Cs_2AgBiBr_6$	
Bond	ρ	$\nabla^2\rho$	ρ	$\nabla^2\rho$
Ag-Br	0.038	0.094	0.038	0.101
Sb/Bi-Br	0.048	0.047	0.045	0.055

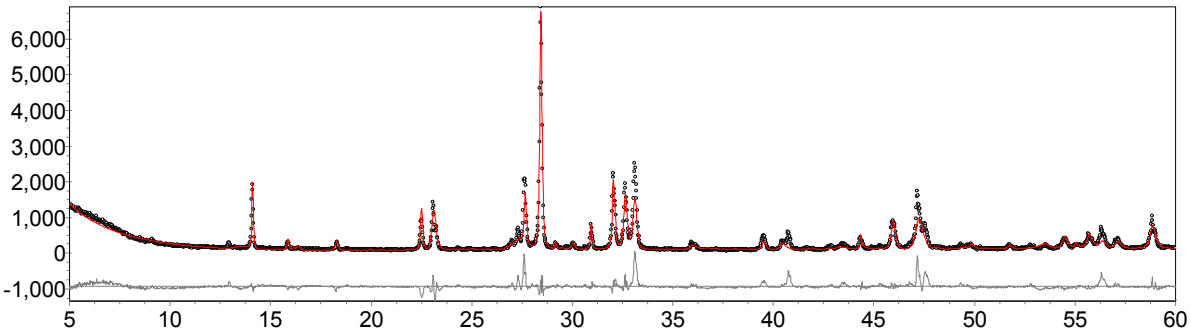

Figure S1. Rietveld refinement for the bulk mixture, showing that the weight ratio of $Cs_2AgSbBr_6$ is ~64%, with a refined lattice parameter of 11.1579(11)Å, which agrees well with single crystal data. Secondary phases include $Cs_3Sb_2Br_9$, Cs_3SbBr_6, Cs_2SbBr_6, Cs_2AgBr_3, $CsAgBr_2$, and unreacted AgBr, CsBr.

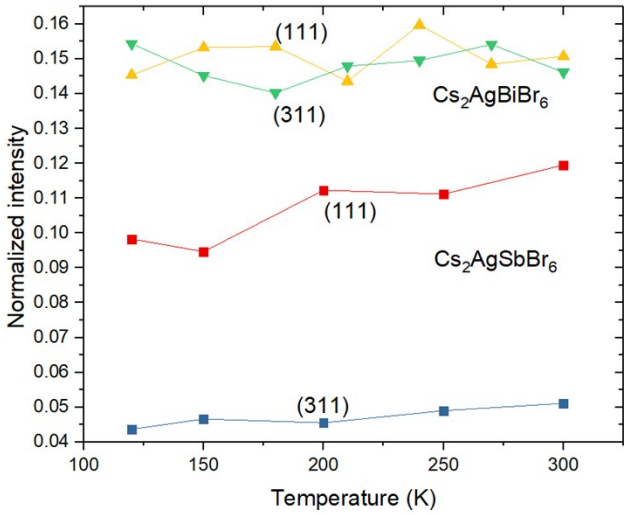

Figure S2. Normalized intensity for superlattice reflections. Normalization is based on the main reflection 200, and absolute intensities were taken by averaging, e.g., the intensity of (200) is taken as the average of (200), (020), (002), (-200), (0-20), and (00-2). Square symbols indicate $Cs_2AgSbBr_6$, triangles represent $Cs_2AgBiBr_6$.

$Cs_2AgSbBr_6$ film/ device characterization

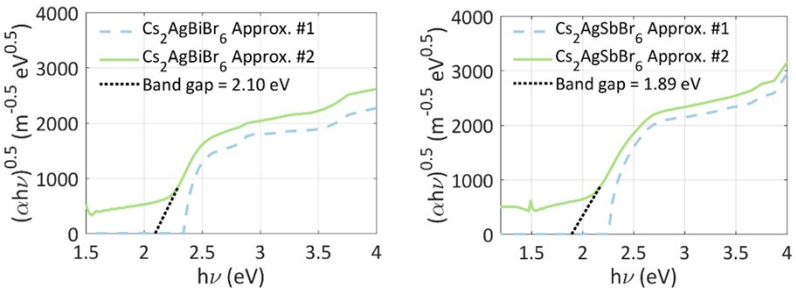

Figure S3. Tauc plots of $Cs_2AgBiBr_6$ and $Cs_2AgSbBr_6$.

Bandgap of $Cs_2AgBiBr_6$ and $Cs_2AgSbBr_6$ thin films were extracted using the method established by Tauc.[1] $Cs_2AgSbBr_6$ shows a lower bandgap in comparison to its Bi counterparts.

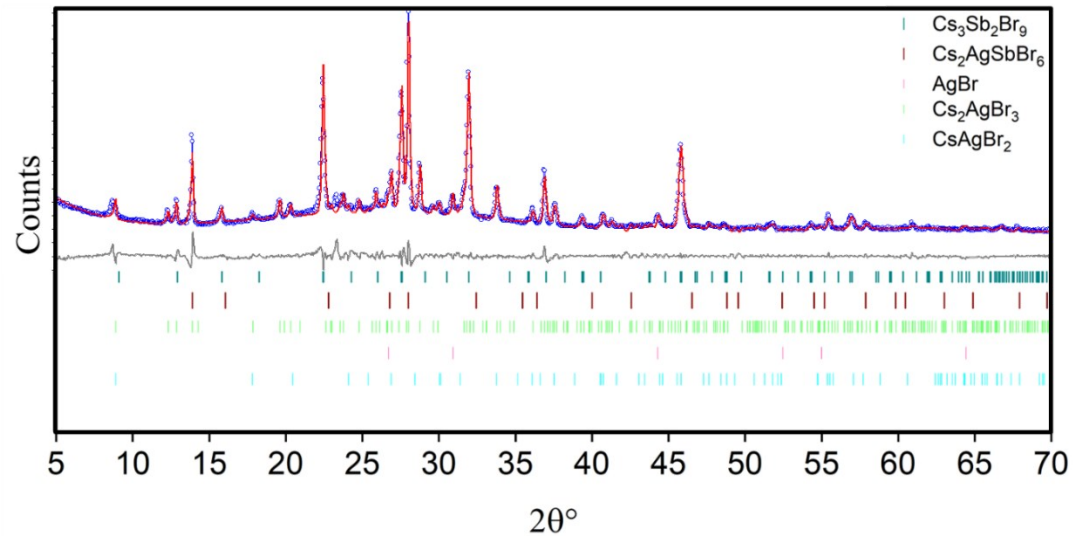

Figure S4. The Pawley refinement for as-synthesized thin-films containing $Cs_2AgSbBr_6$. Blue: experimental; red: calculated; and grey: the differences.

Pawley refinement of obtained $Cs_2AgSbBr_6$ film mixture show three cesium, antimony and bromide based phases, with secondary phases of $Cs_3Sb_2Br_9$, Cs_2AgBr_3 and $CsAgBr_2$, *Rwp* = 7.05%. In addition, a reactant, AgBr was also observed as a minority phase. For the $Cs_2AgSbBr_6$ phase, a space group of $Fm\bar{3}m$ and a = 11.19 Å was obtained from the refinement.

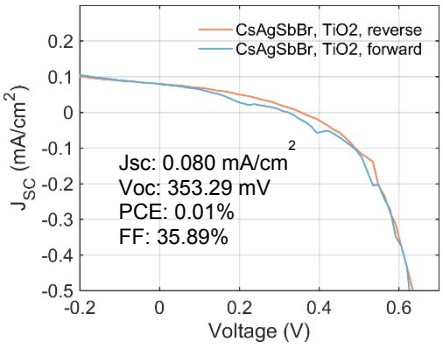

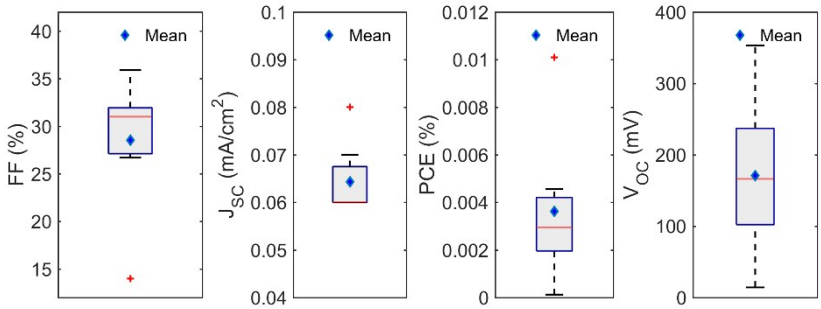

Figure S5. Device performance based on thin-films containing $Cs_2AgSbBr_6$.

References

1 G. M. Sheldrick, *Acta Crystallogr. A*. 2008, **64**, 112–122.

2 G. M. Sheldrick, *Acta Crystallogr. C*, 2015, **71**, 3–8.

3 P. E. Blöchl, *Phys. Rev. B*, 1994, **50**, 17953–17979.

4 G. Kresse, *Phys. Rev. B*, 1999, **59**, 1758–1775.

5 G. Kresse and J. Furthmuller, *Phys. Rev. B*, 1996, **54**, 11169–11186.

6 G. Kresse and J. Furthmuller, *Comput. Mater. Sci.*, 1996, **6**, 15–50.

7 J. Klimes, D. R. Bowler and A. Michaelides, *Phys. Rev. B*, 2011, **83**, 195131.

8 H. J. Monkhorst and J. D. Pack, *Phys. Rev. B*, 1976, **13**, 5188–5192.

9 A. V Krukau, O. A. Vydrov, A. F. Izmaylov and G. E. Scuseria, *J. Chem. Phys.*, 2006, **125**, 224106.

10 Z. Deng, F. Wei, S. Sun, G. Kieslich, A. K. Cheetham and P. D. Bristowe, *J. Mater. Chem. A*, 2016, **4**, 12025–12029.

11 R. F. W. Bader, *Atoms in Molecules: A Quantum Theory*, Clarendon Press, Oxford, UK, 1994.

12 A. Otero-de-la-Roza, E. R. Johnson and V. Luaña, *Comput. Phys. Commun.*, 2014, **185**, 1007–1018.

13 A. H. Slavney, T. Hu, A. M. Lindenberg and H. I. Karunadasa, *J. Am. Chem. Soc.*, 2016, **138**, 2138–2141.